

UDC: 537.312, 621.383

PHOTODETECTORS BASED ON FIELD EFFECT IN POROUS SILICON – REDUCED GRAPHENE OXIDE STRUCTURES

Igor Olenych*  & Andrii Kozak 

Department of Radioelectronic and Computer Systems
Ivan Franko National University of Lviv
50 Dragomanov Street, 79005 Lviv, Ukraine

Olenych, I. and Kozak, A. (2026). Photodetectors Based on Field Effect in Porous Silicon – Reduced Graphene Oxide Structures. *Electronics and Information Technologies*, 33, 191–200.
<https://doi.org/10.30970/eli.33.14>

ABSTRACT

Background. Graphene field-effect transistors (FETs) have high potential for application in sensor electronics as detectors of electromagnetic radiation in a wide spectral range due to the high sensitivity of graphene ambipolar conductivity to local changes in the electric field. The use of a reduced graphene oxide (RGO) film provides cost reduction of photodetectors based on graphene FETs. On the other hand, an additional porous silicon light-absorbing layer can increase their sensitivity due to an increase in surface area.

Materials and methods. Graphene field-effect photodetectors were created by drying a film-forming RGO suspension deposited on the surface of the porous silicon on a silicon substrate, which served as the gate of the FET. Electrical source and drain contacts were formed on the surface of the obtained RGO film. To improve the insulating properties of porous silicon, it was electrochemically oxidized, and an additional layer of Al₂O₃ was deposited. The electrical and photoelectric properties of the created field-effect photodetectors were investigated in DC and AC modes using a white LED and standard optical equipment.

Results. An increase in the conductivity and capacitance of the RGO channel of the FETs was detected under the influence of white light irradiation. Based on the analysis of the drain current dependencies on the gate voltage, it has been established that the efficiency and photosensitivity of the FETs based on the porous silicon and RGO film are increased by the deposition of an additional Al₂O₃ layer on the surface of electrochemically oxidized porous silicon. The maximum sensitivity of the created photodetectors is in the spectral range of 800–900 nm. The response time to white light pulses is about 0.5 ms. Passivation of the porous silicon surface with the oxide film and the Al₂O₃ layer causes an increase in the photosignal relaxation time.

Conclusions. The features of using FETs based on porous silicon structures and RGO film as visible radiation detectors have been investigated. The electrical, spectral, and time characteristics of the created field-effect photodetectors were determined.

Keywords: Graphene field-effect transistor, reduced graphene oxide, porous silicon, photosensitivity.

INTRODUCTION

The unique combination of ultra-high charge carrier mobility in graphene, sensitivity of its electrical conductivity to local changes in the electric field, high transparency, and flexibility provides exceptional prospects for graphene and materials based on *sp*²-bonded



© 2026 Igor Olenych & Andrii Kozak. Published by the Ivan Franko National University of Lviv on behalf of Електроніка та інформаційні технології / Electronics and Information Technologies. This is an Open Access article distributed under the terms of the [Creative Commons Attribution 4.0 License](https://creativecommons.org/licenses/by/4.0/) which permits unrestricted reuse, distribution, and reproduction in any medium, provided the original work is properly cited.

carbon atoms in sensor electronics for creating photodetectors, touch displays, and other next-generation optoelectronic devices [1-3]. Due to the absence of a band gap, graphene absorbs photons of almost any energy, which opens up the possibility of creating photodetectors with a wide spectral range, namely from UV to terahertz radiation. These properties make graphene especially attractive for high-speed telecommunications systems [4, 5], contactless scanning systems [6], and optical sensors in spectroscopic methods of medical diagnostics [7, 8], where both response time and energy efficiency are critical.

Despite the attractiveness of graphene for sensor applications, challenges can be noted that hinder the development of graphene-based devices and their mass industrial application. One obstacle remains scaling up the production of high-quality graphene and ensuring its uniformity over large areas. A solution to this problem may be the use of reduced graphene oxide (RGO), since its manufacturing technology is quite simple and low-cost [9,10]. Field-effect transistors (FETs) based on the RGO film demonstrate high sensitivity to electromagnetic and ionizing radiation [11].

On the other hand, pure graphene demonstrates relatively low quantum efficiency due to its limited absorption capacity (~2.3 % per layer). Therefore, the basic approach to graphene applications in photoelectronics is focused on engineering hybrid structures that combine the charge-sensitive carbon monolayer and a photosensitive material for charge carrier generation. In particular, combining graphene with strong light absorbers, such as perovskites or nanostructured semiconductors and metals, provides a significant increase in photosensitivity due to charge transfer effects or enhancement of local electric fields [12-14]. According to this concept, porous silicon (PS) has high potential for use as a substrate for graphene deposition due to its attractive antireflective properties [15]. The large ratio of surface area to volume of the porous layer provides not only effective absorption of light quanta, but also promotes the deposition of various nature nanoparticles, including RGO [16]. In addition, the nanostructured PS can be used as a supporting layer for the RGO channel of the FETs, owing to its low electrical conductivity [17]. Further improvement of the porous layer dielectric properties increases the efficiency of FETs based on the PS–RGO structures. Therefore, the work aimed to study the relationship between the structural features of the PS-based supporting layer and the electrical and photosensitive properties of the FETs with the RGO film channel.

MATERIALS AND METHODS

Slightly doped silicon wafers with a thickness of 400 μm were used as the substrate and gate of the RGO-based FETs. A thin gold film used as an electrical contact for the gate was thermally deposited on the back surface of the wafers and annealed at a temperature of 600°C for 30 min. On the opposite side of the wafers, the PS layer was formed by the electrochemical method. An ethanolic solution of hydrofluoric acid with a component ratio of $\text{HF}:\text{C}_2\text{H}_5\text{OH} = 1:1$ was used as the electrolyte. The current density and duration of anodic etching were 30 mA/cm^2 and 5 min, respectively. The wafer working surface was illuminated with a Feron HB1 J118 500 W incandescent lamp throughout the entire electrochemical etching process to generate positive charge carriers necessary for the silicon etching chemical reactions. After washing with distilled water, some of the samples were subjected to electrochemical oxidation of the porous layer in a H_2O_2 solution at a current density of 15 mA/cm^2 for 10 min to stabilize the surface and form a thin dielectric film. To improve the dielectric properties of the PS used as an insulating layer between the gate and the RGO channel of the FETs, a 150 nm thick Al_2O_3 film was additionally deposited on the surface of the anodically oxidized porous layer of several samples by RF magnetron sputtering under the conditions described in [11].

The conductive channel of the FETs was formed by air-drying the RGO film-forming suspension deposited on the surface of the insulating layer, obtained by reducing graphene oxide (in the form of an aqueous suspension from Sigma-Aldrich) with hydrazine monohydrate as described in [16]. Silver contacts of source and drain were thermally deposited onto the surface of the formed RGO film at a distance of 1 mm from each other, as shown in Fig. 1.

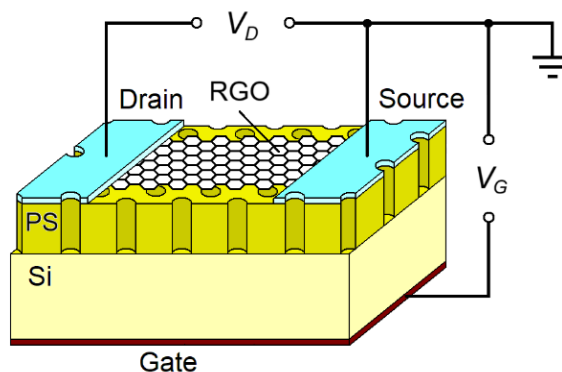


Fig. 1. Schematic representation of the FET based on the PS and RGO film.

The electrical and photoelectric characteristics of the created FETs were studied in DC and AC modes. In particular, the dependencies of the drain current I_D on the bias voltage V_D and the gate voltage V_G were measured using a Siglent SDM 3045 multimeter. The capacitive and resistive characteristics of the RGO channel were investigated using a Hantek 1833C RLC meter in the frequency range of 10^2 – 10^5 Hz. A white LED FYLP–1W–UWB–A with a power of 1 W and a luminous flux of 76 lumens was used to study photoelectric phenomena. The LED emission spectrum has a broad band in the range of 470–600 nm and an intense band with a maximum at about 450 nm. The photoresponse spectra were measured on standard optical equipment and corrected to account for the spectral characteristics of the equipment.

RESULTS AND DISCUSSION

The dependencies of the drain current I_D on the potential difference between the source and drain contacts V_D of the created FETs in the absence of gate voltage ($V_G = 0$) are nonlinear, as shown in Fig. 2. The lowest conductivity was found in the RGO film deposited on the surface of the PS (Si–PS–RGO structure). The RGO film formed on the surface of an anodically oxidized porous layer (Si–PS_{ox}–RGO structure) demonstrates slightly higher conductivity. The highest conductivity of the RGO film is observed in the structure with an additional Al₂O₃ layer (Si–PS_{ox}–Al₂O₃–RGO). Irradiation with white light from the LED FYLP–1W–UWB–A causes an increase in the drain current I_D of the RGO-based FETs. The observed increase in the conductivity of the RGO film is likely caused by the electric field of charge carriers photogenerated in the PS and silicon substrate.

Although the different conductivity values are most likely caused by the different number of carbon nanosheet layers in the RGO film, the nonlinear nature of the I_D – V_D dependencies may have several reasons. Considering that graphene is characterized by ohmic contact resistance with metals [18], it can be assumed that the found nonlinearity is due to both the heterogeneity of the formed films and the influence of the PS layer on the

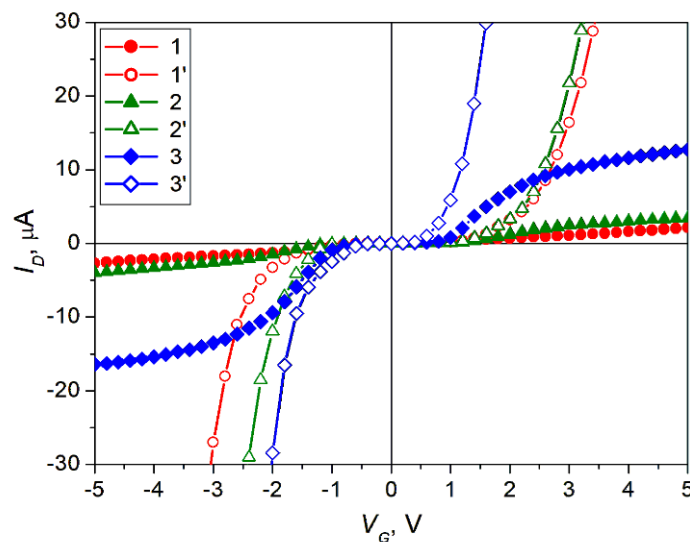
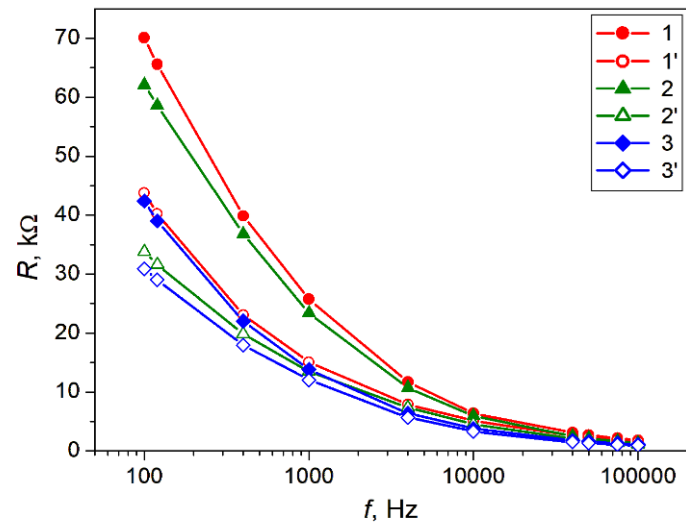


Fig. 2. Dependencies of drain current I_D on bias voltage V_D of the FETs based on the Si-PS-RGO (1,1'), Si-PS_{ox}-RGO (2,2'), and Si-PS_{ox}-Al₂O₃-RGO (3,3') structures measured in the dark (1,2,3) and under irradiation with white light (1',2',3') at the gate voltage $V_G = 0$.

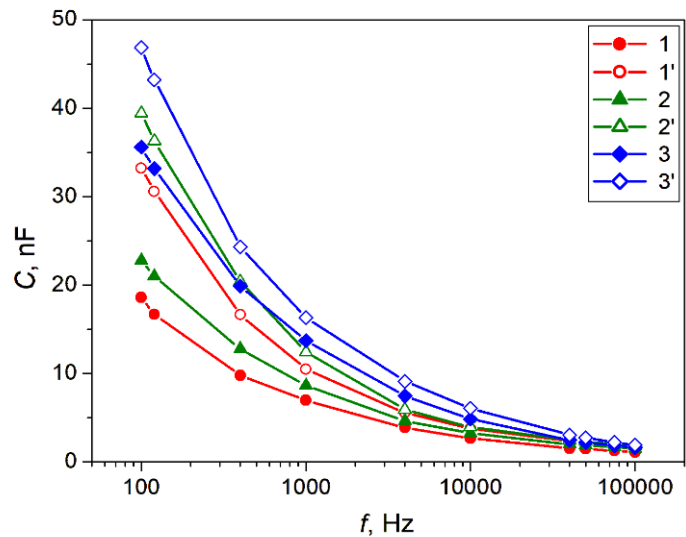
RGO conductivity. First of all, the electrical properties of the RGO film depend not only on the conductivity of the 2D carbon nanoparticles but also on the electrical barriers between them, which are likely formed due to the presence of a surfactant in the film-forming suspension [16]. In addition, since porous silicon is not a perfect insulator [15], charge carriers injected from the PS should not be ignored. Finally, due to the structural imperfection of the PS dielectric coating, the electrical conductivity of the RGO film can also be affected by charge carriers localized on electrically active defects and the interface with the RGO.

The capacitive and resistive properties of the created FETs were investigated in the AC mode to obtain additional information about the charge transfer processes in the RGO film. **Fig. 3** shows the frequency dependencies of the internal resistance and capacitance of the RGO film, measured between the source and drain contacts. A decrease in electrical characteristics was detected with increasing frequency from 100 Hz to 100 kHz. A decrease in resistance and an increase in capacitance of the RGO film were also found under irradiation of the working surface of the field-effect photodetectors. The observed dispersion of the electrical characteristics of the RGO channel of the FETs may further support the assumption of inhomogeneities in the RGO film formed from carbon nanosheets.

Dependencies of the drain current I_D on the gate voltage V_G were measured to evaluate the efficiency of the created FETs based on the RGO film. The obtained I_D - V_G curves at $V_D = \pm 1.5$ V are shown in **Fig. 4**. The drain current increases linearly with the change in gate voltage from approximately 0 to -4 V for the bias voltage of $V_D = 1.5$ V. Similarly, the conductivity of the RGO channel of the FETs increases almost linearly with increasing V_G from 1.5 to 4 V for $V_D = -1.5$ V. The minimum conductivity of the RGO-based FETs at about 1 V gate voltage is caused by the features of the graphene band structure in the form of Dirac cones and is associated with the charge neutrality point, which divides the conductivity profile into hole and electron components [19].



a)



b)

Fig 3. Frequency dependencies of the internal resistance (a) and capacitance (b) of the RGO channel of the FETs based on the Si-PS-RGO (1,1'), Si-PS_{ox}-RGO (2,2'), and Si-PS_{ox}-Al₂O₃-RGO (3,3') structures measured in the dark (1,2,3) and under irradiation with white light (1',2',3') at the gate voltage of $V_G = 0$.

Analysis of the measured I_D-V_G dependencies shows that the FET based on the Si-PS_{ox}-Al₂O₃-RGO structure, which demonstrates the largest range of change in drain current when the gate voltage changes, has the highest efficiency. The revealed features of the electrical characteristics of the FETs based on the PS and RGO film may be due to the different quality of the insulating layers, since the performance of graphene field-effect devices depends significantly on defects in the supporting dielectric layer [20].

As a result of irradiation of the FETs with white light, an increase in the drain current I_D was observed at a bias voltage of $V_D = \pm 1.5$ V. The highest photosensitivity to white light is demonstrated by the structure with the additional Al₂O₃ layer, probably due to the higher FET efficiency. The small thickness of the transparent to visible light Al₂O₃ layer does not

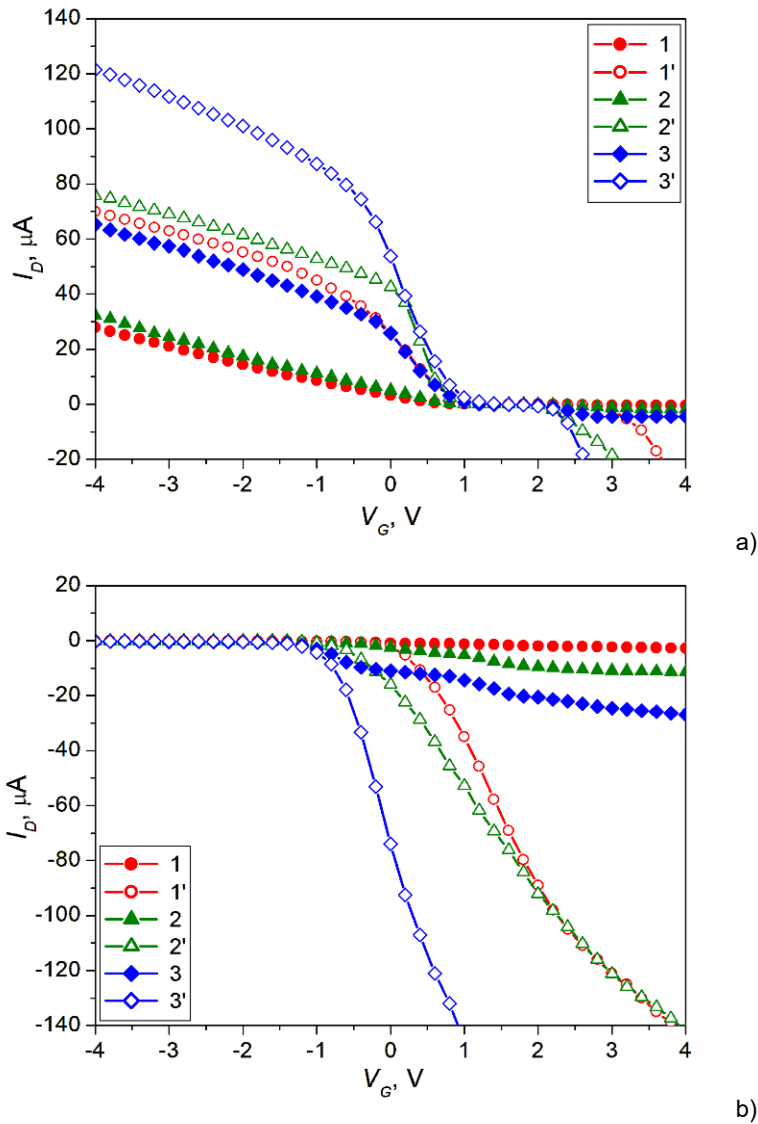


Fig 4. Dependencies of drain current I_D on gate voltage V_G of the FETs based on the Si-PS-RGO (1,1'), Si-PS_{ox}-RGO (2,2'), and Si-PS_{ox}-Al₂O₃-RGO (3,3') structures measured in the dark (1,2,3) and under irradiation with white light (1',2',3') at the bias voltages $V_D = 1.5$ V (a) and $V_D = -1.5$ V (b).

significantly affect the sensitivity of the proposed field-effect photodetector. In addition, improved passivation of the PS surface with the Al₂O₃ layer can reduce the rate of photogenerated charge carrier recombination. An additional argument in favor of this hypothesis is the increase in the relaxation time of the photoresponse to white light pulses, as shown in the inset of **Fig. 5**. In general, the analysis of the photoresponse kinetics of the created photodetectors revealed almost the same rate of increase in the photosignal and different times of its decay when excited by light pulses with a duration of 1 ms.

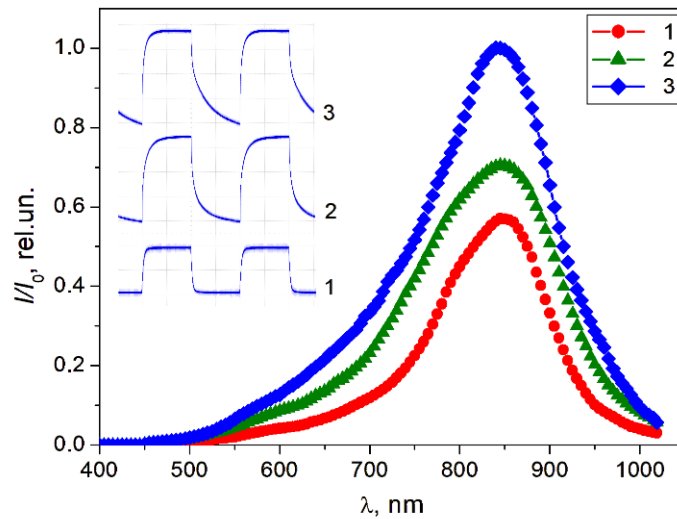


Fig 5. Photoresponse spectra of the FETs based on the Si-PS-RGO (1), Si-PS_{ox}-RGO (2), and Si-PS_{ox}-Al₂O₃-RGO (3) structures. Inset: response kinetics of the photodetectors to white light pulses.

The spectral characteristic of the field-effect photodetectors depends on the light-absorbing properties of the PS and silicon substrate. The photosensitivity spectra of the RGO-based FETs are characterized by a broad band with a maximum in the 800–900 nm range, similar to a silicon photodiode (see Fig. 5).

CONCLUSION

As a result of studying the electrical and photoelectric characteristics of the FETs based on the PS and RGO film, the features of their use as photodetectors have been established. It was revealed that irradiation of FETs with white light causes an increase in the conductivity of the RGO channel in both DC and AC modes. In addition, the efficiency and photosensitivity of the created FETs were increased due to the deposition of an additional Al₂O₃ layer on the surface of the anodically oxidized PS. Moreover, the improved passivation of the PS surface with the Al₂O₃ layer increases the relaxation time of the photoresponse to white light pulses. The response time of the field-effect photodetectors is about 0.5 ms. It has been established that the photosensitivity of FETs based on the RGO film is maximum in the range of 800–900 nm.

ACKNOWLEDGMENTS AND FUNDING SOURCES

This work was supported by the Ministry of Education and Science of Ukraine [0124U000982].

COMPLIANCE WITH ETHICAL STANDARDS

The authors declare that the research was conducted in the absence of any conflict of interest.

AUTHOR CONTRIBUTIONS

Conceptualization, [IO]; methodology, [IO, AK]; investigation, [IO, AK]; writing – original draft preparation, [IO, AK]; writing – review and editing, [IO]; visualization, [IO].

All authors have read and agreed to the published version of the manuscript.

REFERENCES

- [1] Zhang, X., Liu, X., Huang, Y., Sun, B., Liu, Z., Liao, G., & Shi, T. (2023). Review on flexible perovskite photodetector: processing and applications. *Front. Mech. Eng.*, 18, 33. <https://doi.org/10.1007/s11465-023-0749-z>
- [2] Esteghamat, A. & Akhavan, O. (2023). Graphene as the ultra-transparent conductive layer in developing the nanotechnology-based flexible smart touchscreens. *Microelectronic Engineering*, 267-268, 111899. <https://doi.org/10.1016/j.mee.2022.111899>
- [3] Ishida, S., Anno, Y., Takeuchi, M., Matsuoka, M., Takei, K., Arie, T., & Akita, S. (2015). Highly photosensitive graphene field-effect transistor with optical memory function. *Sci. Rep.*, 5, 15491. <https://doi.org/10.1038/srep15491>
- [4] Romagnoli, M., Sorianello, V., Midrio, M., Koppens, F.H.L., Huyghebaert, C., Neumaier, D., Galli, P., Templ, W., D'Errico, A., & Ferrari, A.C. (2018). Graphene-based integrated photonics for next-generation datacom and telecom. *Nature Reviews Materials*, 3, 392-414. <https://doi.org/10.1038/s41578-018-0040-9>
- [5] Ding, Y., Cheng, Z., Zhu, X., Yvind, K., Dong, J., Galili, M., Hu, H., Mortensen, N., Xiao, S., & Oxenløwe, L. (2020). Ultra-compact integrated graphene plasmonic photodetector with bandwidth above 110 GHz. *Nanophotonics*, 9(2), 317-325. <https://doi.org/10.1515/nanoph-2019-0167>
- [6] Liu, J., Li, X., Jiang, R., Yang, K., Zhao, J., Khan, S. A., He, J., Liu, P., Zhu, J., & Zeng, B. (2021). Recent Progress in the Development of Graphene Detector for Terahertz Detection. *Sensors*, 21(15), 4987. <https://doi.org/10.3390/s21154987>
- [7] Suvamaphaet, P., & Pechprasarn, S. (2017). Graphene-Based Materials for Biosensors: A Review. *Sensors*, 17(10), 2161. <https://doi.org/10.3390/s17102161>
- [8] Baruah, A., Newar, R., Das, S., Kalita, N., Nath, M., Ghosh, P., Chinnam, S., Sarma, H., & Narayan, M. (2024). Biomedical applications of graphene-based nanomaterials: recent progress, challenges, and prospects in highly sensitive biosensors. *Discover Nano*, 19, 103. <https://doi.org/10.1186/s11671-024-04032-6>
- [9] Pei, S. & Cheng, H.M. (2012). The reduction of graphene oxide. *Carbon*, 50, 3210–3228. <https://doi.org/10.1016/j.carbon.2011.11.010>
- [10] Abakumov, A.A., Bychko, I.B., Voitsihovska, O.O., Rudenko, R.M., & Strizhak, P.E. (2024). Tuning the surface area of reduced graphene oxide by modulating graphene oxide concentration during hydrazine reduction. *Materials Letters*, 354, 135417. <https://doi.org/10.1016/j.matlet.2023.135417>
- [11] Olenych, I.B., Monastyrskii, L.S., Sokolovskii, B.S., Turko, B.I., & Dzendzelyuk, O.S. (2025). Field-effect transistors based on reduced graphene oxide film for photo and radiation detectors. *Sensor Electronics and Microsystem Technologies*, 22(2), 19–26, (in Ukrainian). <https://doi.org/10.18524/1815-7459.2025.2.333193>
- [12] Abbas, K., Ji, P., Ullah, N., Shafique, S., Zhang, Z., Ameer, M.F., Qin, S., & Yang, S. (2024). Graphene photodetectors integrated with silicon and perovskite quantum dots. *Microsyst. Nanoeng.*, 10, 81, <https://doi.org/10.1038/s41378-024-00722-4>
- [13] Thai, K.Y., Park, I.J., Kim, B.J., Hoang, A.T., Na, Y., Park, C.U., Chae, Y., & Ahn, J.-H. (2021). MoS₂/Graphene Photodetector Array with Strain-Modulated Photoresponse up to the Near-Infrared Regime. *ACS Nano*, 15(8), 12836–12846. <https://doi.org/10.1021/acsnano.1c04678>

- [14] Ye, M., Zha, J., Tan, C., & Crozier, K.B. (2021). Graphene-based mid-infrared photodetectors using metamaterials and related concepts. *Appl. Phys. Rev.* 8, 031303. <https://doi.org/10.1063/5.0049633>
- [15] Bisi, O., Ossicini, S., & Pavesi, L. (2000). Porous silicon: a quantum sponge structure for silicon based optoelectronics. *Surf. Sci. Rep.*, 38, 1–126. [https://doi.org/10.1016/S0167-5729\(99\)00012-6](https://doi.org/10.1016/S0167-5729(99)00012-6)
- [16] Olenych, I. B. & Horbenko, Yu. Yu. (2024). Electrical and photoelectric properties of hybrid structures based on reduced graphene oxide and Pd-doped porous silicon. *Mol. Cryst. Liq. Cryst.*, 768, 135-144. <https://doi.org/10.1080/15421406.2023.2235191>
- [17] Olenych, I.B., Horbenko, Y.Y., & Sokolovskii, B.S. (2024). Effect of supporting layer on electrical characteristics of field-effect transistor based on reduced graphene oxide film. *Mol. Cryst. Liq. Cryst.*, 768(11), 426–435. <https://doi.org/10.1080/15421406.2024.2353960>
- [18] Xia, F., Perebeinos, V., Lin, Y.-M., Wu, Y., & Avouris P. (2011). The origins and limits of metal graphene junction resistance. *Nature Nanotechnology*, 6(3), 179–184. <https://doi.org/10.1038/nnano.2011.6>
- [19] Zhan, D., Yan, J., Lai, L., Ni, Z., Liu, L., & Shen, Z. (2012). Engineering the Electronic Structure of Graphene. *Adv. Mater.*, 24, 4055–4069. <https://doi.org/10.1002/adma.201200011>
- [20] Imamura, G. & Saiki, K. (2015). Modification of Graphene/SiO₂ Interface by UV-Irradiation: Effect on Electrical Characteristics. *ACS Appl. Mater. Interfaces*, 7, 2439–2443. <https://doi.org/10.1021/am5071464>
-

ФОТОДЕТЕКТОРИ НА ОСНОВІ ЕФЕКТУ ПОЛЯ У СТРУКТУРАХ ПОРУВАТИЙ КРЕМНІЙ – ВІДНОВЛЕНИЙ ОКСИД ГРАФЕНУ

Ігор Оленич* , Андрій Козак 

Кафедра радіоелектронних і комп'ютерних систем
Львівський національний університет імені Івана Франка,
вул. Драгоманова 50, 79005 м. Львів, Україна

АНОТАЦІЯ

Вступ. Завдяки високій чутливості біполярної провідності графену до локальної зміни електричного поля, графенові польові транзистори мають високий потенціал для застосування у сенсорній електроніці, зокрема як детектори електромагнітного випромінювання у широкому спектральному діапазоні. Використання плівки відновленого оксиду графену (ВОГ) дає змогу знизити вартість фотодетекторів на основі графенових польових транзисторів, тоді як додатковий світлопоглинаючий шар поруватого кремнію може забезпечити підвищення їхньої чутливості завдяки збільшенню площі поверхні.

Матеріали та методи. Фоточутливі графенові польові транзистори отримано висушуванням плівкоутворювальної суспензії ВОГ, нанесеної на поверхню поруватого кремнію на кремнієвій підкладці, що слугувала затвором польового транзистора. На поверхні утвореної плівки ВОГ сформовано електричні контакти витоку та стоку. Для покращення ізоляційних властивостей поруватого кремнію його було електрохімічно окиснено та осаджено додатковий шар Al₂O₃. Електричні та фотоелектричні властивості створених польових транзисторів досліджено у режимах постійного та

змінного струму з використанням світлодіодного діода білого світла і стандартного оптичного обладнання.

Результати. Виявлено збільшення провідності та ємності ВОГ-каналу польових транзисторів за впливу опромінення білим світлом. На основі аналізу залежностей струму стоку від напруги затвора встановлено, що ефективність і фоточутливість польових транзисторів на основі поруватого кремнію та плівки ВОГ збільшується завдяки осадженню додаткового шару Al_2O_3 на поверхню електрохімічно окисненого поруватого кремнію. Максимум чутливості створених фотодетекторів знаходиться у спектральному діапазоні 800–900 нм. Час відгуку на імпульси білого світла становить близько 0,5 мс. Пасивація поверхні поруватого кремнію оксидною плівкою та шаром Al_2O_3 зумовлює збільшення часу релаксації фотосигналу.

Висновки. Досліджено особливості використання польових транзисторів на основі поруватого кремнію та плівки ВОГ як детекторів видимого випромінювання. Визначено електричні, спектральні та часові характеристики створених фотодетекторів.

Ключові слова: Графеновий польовий транзистор, відновлений оксид графену, поруватий кремній, фоточутливість.